Bull. Mater. Sci., Vol. 35, No. 2, April 2012, pp. 197–202. © Indian Academy of Sciences.

Diffuse phase transition, piezoelectric and optical study of $Bi_{0.5}Na_{0.5}TiO_3$ ceramic

B PARIJA, T BADAPANDA[†*], V SENTHIL, S K ROUT[‡] and S PANIGRAHI

Department of Physics, National Institute of Technology, Rourkela 769 008, India
[†]Department of Physics, C V Raman College of Engineering, Bhubaneswar 752 054, India
[‡]Department of Applied Physics, Birla Institute of Technology, Mesra, Ranchi 835 215, India

MS received 14 November 2010; revised 16 June 2011

Abstract. **Bismuth sodium titanate, $Bi_{0.5}Na_{0.5}TiO_3$ (BNT) is considered to be an excellent candidate for a key material of lead-free dielectric ceramics. In this study, we propose the dielectric and optical study of single phase BNT powder prepared by solid-state reaction route. The phase formation and structural study were done by X-ray diffraction (XRD) which shows well developed crystallite with a pure perovskite phase. The ceramic was sintered at different temperatures from 1050°C to 1175°C to study the effect of sintering temperature on the morphology and density. It was found that the sample sintered at 1150°C shows the highest density. The microstructure of the ceramic was investigated by scanning electron microscopic (SEM) technique. The temperature-dependent dielectric study of the sample sintered at 1150°C was done in the frequency range of 50 kHz–1 MHz which shows a diffuse phase transition. The piezoelectric constant (d_{33}) was found to be 41 pCN^{-1}. The P–E hysteresis loop confirms the ferroelectric behaviour in the ceramic. The UV–Vis spectrum indicated that the $Bi_{0.5}Na_{0.5}TiO_3$ ceramic has an optical band gap of 2·94 eV.**

Keywords. **Dielectric; piezoelectric; diffuse phase transition; optical study.**

1. Introduction

Recently lead was expelled from many commercial applications and materials owing to its toxicity. Ferroelectric lead zirconate titanate (PZT) ceramics were extensively used for many industrial purposes due to their high dielectric and electromechanical properties. However, the toxicity of lead oxide and its high vapour pressure during the sintering process not only causes environmental pollution but also generate instability in composition and electrical properties of products. Therefore, it is necessary to develop environment-friendly lead-free piezoelectric ceramics, which have become one of the main trends in the present development of piezoelectric materials (Smolenskii *et al* 1961). Although there was a concerted effort to develop lead-free piezoceramics, no effective alternative to PZT was yet found. Bismuth sodium titanate ($Bi_{0.5}Na_{0.5}$)TiO_3 (abbreviated as BNT) was considered to be an excellent candidate as a key material of lead-free piezoelectric ceramics and attracted considerable attention in the past few decades. It was studied continually by several researchers in recent years (Zvirgzds *et al* 1980; Takenaka and Takenaka 1998; Walsh and Schulze 2004).

BNT can be synthesized by chemical co-precipitation method, sol–gel method, hydrothermal route and solid-state reaction method (Kuharuangrong and Suhulze 1996; Herabut and Safari 1997; Jiang *et al* 1997; Said and Mercurio 2001; Lenka *et al* 2002). Solid-state reaction processing route to ceramic powders involves heating reactants, so it is an easiest and one of the popular methods. Solid-state synthesis sometimes called as 'conventional technique'. This method helps to control particle size and morphology (Diasa *et al* 1999). In this study, the solid-state reaction synthesis, the effect of sintering temperature on microstructure, dielectric properties and the optical study of calcined BNT were investigated.

2. Experimental

We have used Bi_2O_3 (S.P. Fine Chemical Ltd., Mumbai), Na_2CO_3 (Loba Chemicals Pvt. Ltd., Mumbai) and TiO_2 (Merck Specialties Pvt. Ltd., Mumbai) as the starting materials in the fabrication of BNT ceramic. All the precursors have purity of 99·9%. The oxide and carbonate powders were weighed according to their respective stoichiometric proportions, and then mixed by ball mill with zirconia media in acetone medium for a period of 12–16 h. The purpose of ball milling was strictly to create a homogeneous mixture of the powders, and not to reduce particle size. After mixing, the suspensions were poured into Pyrex dishes and acetone was evaporated from the mixture. The dried mixture was calcined at 850°C for 2 h at a rate of 300°C/h to burn out the carbonate, and to allow the perovskite structure to form the individual components. Before calcining, thermogravimetric analysis (TGA) of the powdered mixture of the starting materials was carried out using a thermogravimetric analyser (Netzsch) with increasing the temperature at a rate

*Author for correspondence (badapanda.tanmaya@gmail.com)

of 10°C/min. XRD analysis was carried out with an X-ray diffractometer (XRD, X-Pert high score) using monochromatic CuKα radiation. The deflection range was 20–70° with a step size of 0·5°/min. The calcinated powders were granulated with an organic binder poly vinyl alcohol (5 wt.%). To get uniform and fine grain, the granules were passed through 73 μm sieve. The residues after sieving were again crushed in an agate mortar and passed through the sieve. The process was repeated until all the granules become less than 73 μm. Then pellets of diameter 10 mm and thickness 1 mm by a cylindrical steel dia was prepared in hydraulic uniaxial press. Since density of the electronic ceramic is a very sensitive parameter and that directly affects their properties, therefore, proper sintering of the pellet is essential for electrical measurements. The pellets were sintered at 1050, 1075, 1100, 1125, 1150 and 1175°C for 4 h and then density was measured by Archimedes principle method.

The relative density, ρ_γ of a BNT disk is given by,

$$\rho_\chi = \frac{\rho_m}{\rho_t} \times 100, \tag{1}$$

where ρ_t and ρ_m are the theoretical density and the measured density, respectively.

The experimental bulk density and apparent porosity were measured by using Archimedes principle;

$$\mathrm{BD} = D/(W-I), \tag{2}$$

$$\mathrm{AP} = (W-D)/(W-I), \tag{3}$$

where BD; bulk density, AP; apparent porosity, D; dry weight, W; shocked weight and I; suspended weight.

The sintered pellets were taken SEM and EDX for grain size, morphology and elemental analysis using JSM T330 scanning electron microscopy (JEOL, USA). Using the linear intercept method presented by Fullman (1953), the average grain size in BNT disk is given by,

$$G = 1.56\frac{\sum_{i=1}^{n} L_i}{N_B}, \tag{4}$$

where, G, n, L_i, and N_B, each represent the average grain size in the disk, the total number of straight lines drawn on the SEM image, the length of the i_{th} straight line drawn on the SEM image, and the total number of grain boundaries, which are intersected by all of the straight lines drawn on the SEM image, respectively. The highest density sample was taken for dielectric study after pasting the silver as an electrode on both the disk side followed by heat treatment at 300°C (15 min) for better conductance. The dielectric measurements were carried out in the frequency range from 50 Hz to 1 MHz using a LCR tester (Hioki, Japan) connected to computer. The dielectric data were collected every 5°C, keeping a heating rate of 1°C/min. Ferroelectric hysteresis measurements (PE loop) were traced at room temperature for the poled and unpoled samples using modified Sawyer–Tower circuit by applying a.c. fields. The piezoelectric coefficient d_{33} was measured using a piezo-d_{33} meter (NTPL\018\08-09, NIT, Rourkela, Orissa). The pooling field was 3 kV/mm, because the coercive field of BNT, E_c = 7·3 kV/mm. Generally, the pooling field should be less than the coercive field (E_c) at room temperature, otherwise breakdown occurs, but here as the polling temperature was 110°C for 20 min, hence the pooling field was 3 kV/mm.

The optical properties were taken absorbance data using diffusive reflectance mode by SHIMAZDU 2450 UV/Vis spectrophotometer. A $BaSO_4$ was used as a reference, on which fine-ground powders of the sample were pressed. The spectra were recorded at room temperature in the wavelength range of 200–700 nm.

3. Results and discussion

3.1 *X-ray diffraction study*

Figure 1 shows the XRD pattern of BNT powder calcined at 850°C for 2 h. The XRD analysis of the calcined powder shows that the samples (BNT) were single phase and maintain the rhombohedral structure with space group R3C. X-ray pattern from JCPDS reference (file no. 36–0340) was also plotted for comparison. A systematic shift of peaks in the XRD pattern of BNT was most likely due to the error in zero positioning of X-ray instrument. Nevertheless, the relative intensity and positions for X-ray peaks of the sample agreed with the reference pattern. The lattice parameters were found to be a = 5·5158 Å, b = 5·5158 Å, c = 13·46 Å and the cell volume was found to be 176·5 Å^3.

3.2 *Effect of sintering temperature*

In this study, the densities of sintered BNT ceramics at 1050, 1075, 1100, 1125, 1150 and 1175°C for 4 h, were

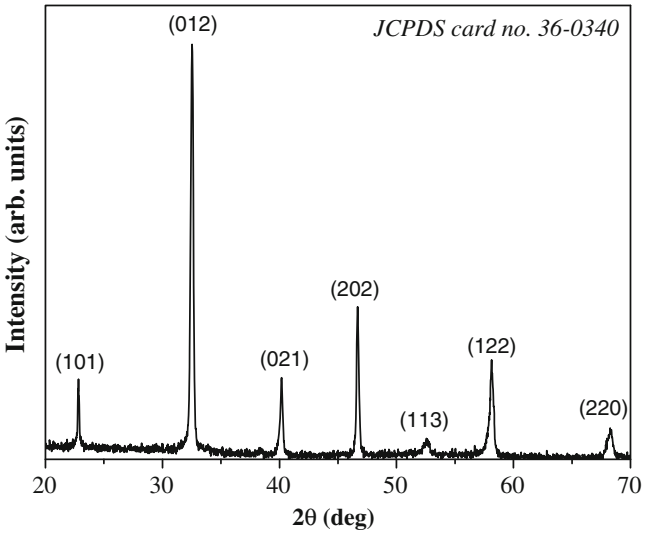

Figure 1. Room temperature XRD of $Bi_{0.5}Na_{0.5}TiO_3$ powder calcined at 850°C for 2 h.

found to be 58, 54, 64, 82, 90 and 94% of their theoretical density, respectively. Figure 2 shows the density and apparent porosity of the sintered samples at various temperatures. This indicates that the sintering temperature of 1150°C for 4 h yielded the highest density of the sintered ceramics. However, the sintering temperature has an influence on the morphology and microstructure of sintered BNT ceramics. It was found that the average grain size of sintered BNT ceramics at 1050–1150°C for 4 h was approximately 1–5 μm. Figure 3(a–f) shows SEM micrographs of BNT ceramics sintered at 1050, 1075, 1100, 1125, 1150 and 1175°C for 4 h. The particles were agglomerate and basically irregular in shape (figures 3a, b). Some spherical particles have diameter ranging from 0·2 to 1·0 μm. A sintered surface ceramic with fine grain and non-uniform microstructure was obtained in BNT ceramics (figures 3c, d), with average grain size ranging from 1 to 5 μm. It can be concluded that, lower sintering temperature with longer sintering time produced smaller grain size ceramics. As shown in figure 2, the density of the BNT ceramics increased sharply as the sintering temperature increased from 1075°C to 1150°C and the porosity decreases with increase in sintering temperature. A maximum density of 5·72 g/cm^3, which was 94% of the theoretical density, was obtained for samples sintered at 1150°C. However, the density drops

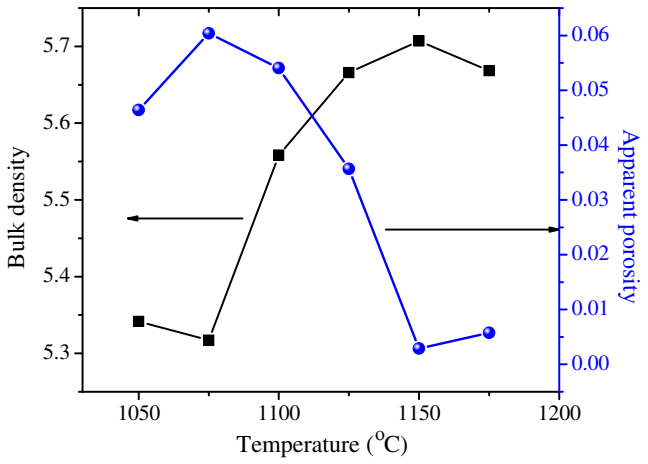

Figure 2. Bulk density and apparent porosity at different temperatures of BNT pellets.

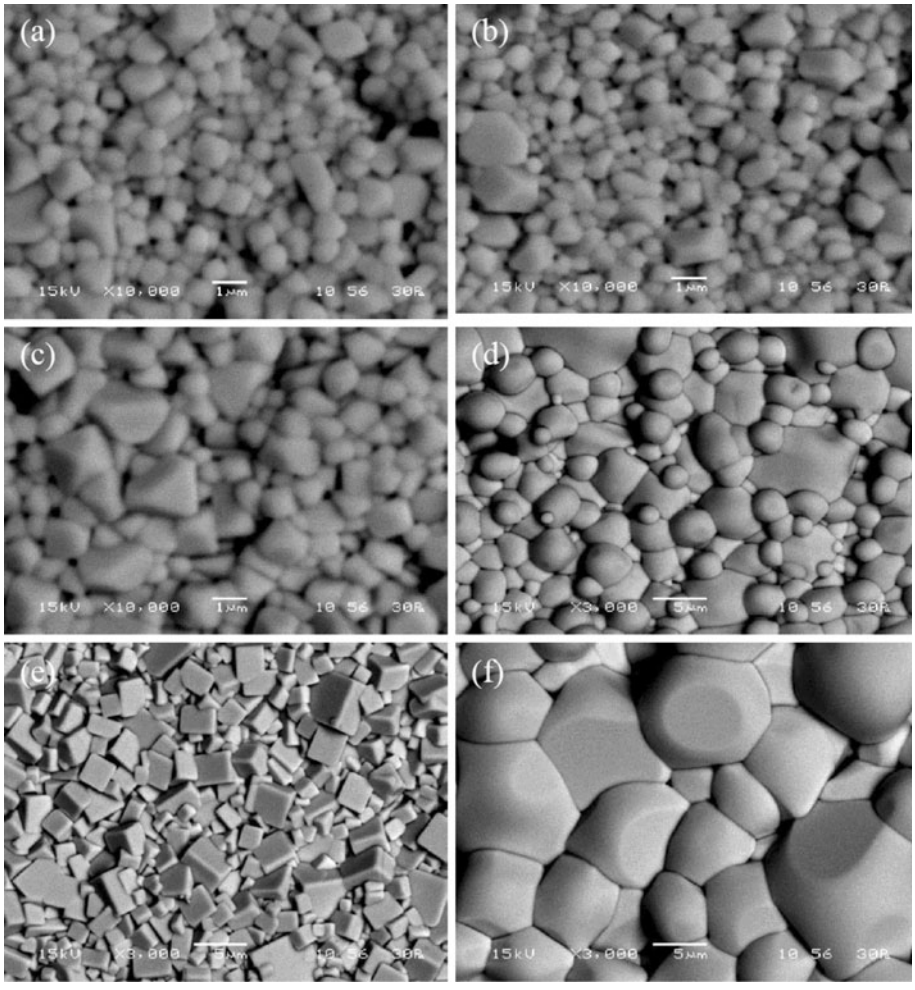

Figure 3. SEM of BNT pellets sintered at: (**a**) 1050°C; (**b**) 1075°C; (**c**) 1100°C; (**d**) 1125°C; (**e**) 1150°C and (**f**) 1175°C for 4 h.

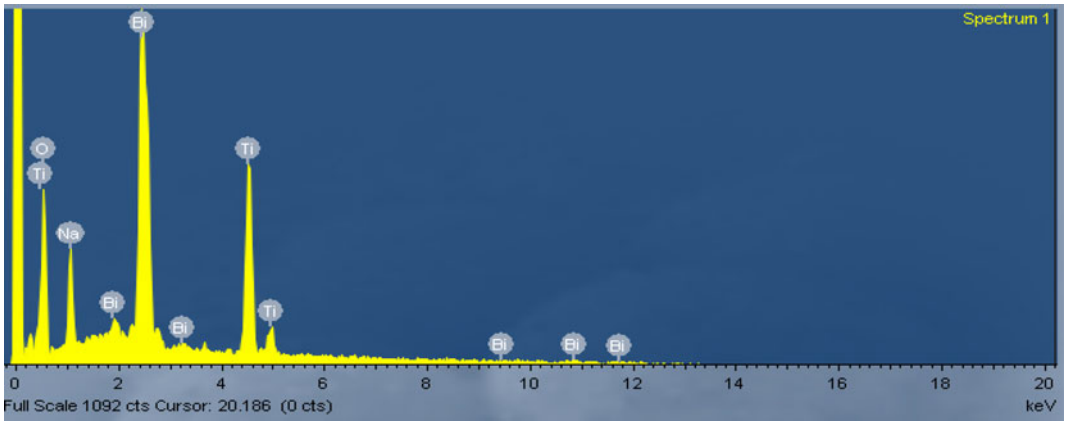

Figure 4. Elemental analysis (EDAX) of BNT pellet.

when the temperature was further increased to 1175°C. The densification behaviour of the BNT ceramics at different sintering temperatures can be explained in terms of defect chemistry and the creation of oxygen vacancies. At lower sintering temperatures, the number of oxygen vacancies is small and the ability of atoms to diffuse is also small which results in poor densification. The lower density of the BNT ceramics sintered at 1050°C is due to poor atomic diffusion and insufficient sintering of the ceramics. It was demonstrated both theoretically and experimentally that the number of vacancies increases with increase in sintering temperature. As a result, better atomic diffusion during the sintering process occurs and thus, promotes densification. However, the low density at a higher sintering temperature of 1175°C may be due to evaporation of the volatile alkali metal (Zhen and Li 2006; Marcos *et al* 2007; Zhao *et al* 2007). The elemental composition of the BNT ceramic was confirmed by EDAX spectrum as shown in figure 4.

Theoretically, if the sintering temperature goes below the critical temperature, the relative density will also increase along with the temperature. This result can probably be attributed to the fact that with the solid phase sintering, the atomic diffusion promotes the densification of the BNT disk, and this process may be enhanced by increasing the temperature. However, as the sintering temperature exceeds the critical temperature, the relative density decreases with increase in temperature. This is due to the fact that the coarsening process may dominate as the sintering temperature is higher than the critical temperature, and reduce the driving force for densification (Rahaman 2003). This trend was observed by Liu *et al* (2009). Further, Watcharapasorn *et al* (2007) showed that increasing the sintering temperature only had an effect on increasing the grain size without appreciably affecting its density.

3.3 *Dielectric study*

Temperature dependence of relative dielectric constant at measuring frequencies of 50 kHz, 100 kHz, 500 kHz and 1 MHz is shown in figure 5. It can be seen from

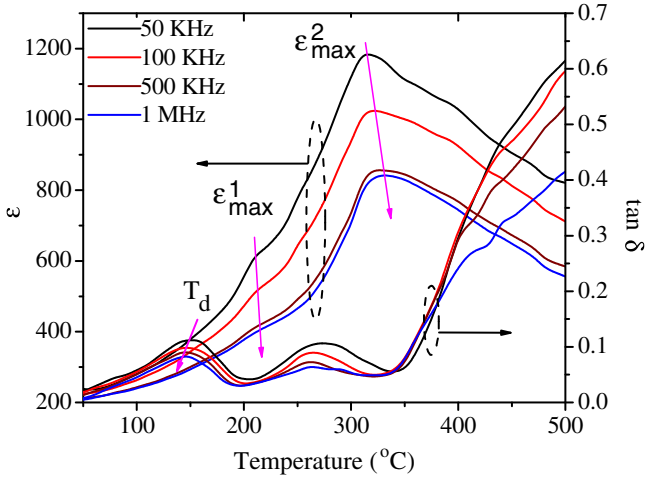

Figure 5. Temperature dependence on dielectric constant ε_r and loss tangent (tan δ) of BNT ceramic.

figure 5 that the phase transformation process of BNT is complex. There are two ε_r peaks in the graph, which appear at 210 and 316°C, respectively, and we call these two temperatures as characteristic temperature (abbreviated as T_c). The conventional explanation, regarding this phenomenon, is that different phase transformation process occurs at two T_c; ferroelectric–antiferroelectric transformation process at 210°C and antiferroelectric–paraelectric transformation process at 316°C (Kimura *et al* 2004). But new proofs show that there is no antiferroelectric phase between the two T_c. It is the stage where trigonal and tetragonal states coexist, with polar micro-domains altering.

Figure 5 shows the temperature dependencies of the tan δ for pure BNT ceramics at different frequencies. The depolarization temperature (T_d) near 150°C can be derived from the temperature of the tan δ first peak at a certain frequency and, accordingly, depends on the determining frequency. Hiruma *et al* (2006, 2008) asserted that for fully-poled ceramic samples in a sufficiently high electric field, the first sharp peak of tan δ had no frequency dependence and that the T_d obtained using this method corresponded

to that determined from the variations of electromechanical coupling constant k_p with temperature. There were reports that above a critical field, the d.c. bias electric field induced a transition from the relaxor to the long-range ferroelectric phase in La-modified PZT ceramics (Perantie *et al* 2008).

The relative dielectric constant increases slowly with the increasing temperature below 210°C, and more rapidly above 210°C until the temperature T_{max} of maximum dielectric constants ε^1_{max}. Rapid increases in ε_r occurred near 316°C on heating, which is the structural phase transition temperature from the rhombohedral to the tetragonal phase. Another feature in figure 5 is that the temperature T_{max} increases with measuring frequencies; they are: 316, 321, 326 and 331°C at frequencies of 50 kHz, 100 kHz, 500 kHz and 1 MHz, respectively. Also, the value of the relative dielectric constant decreases as the measuring frequency increases showing evidence of a diffuse phase transition with a straight frequency dispersion occurring around the temperature T_{max}.

Peak broadening may be quantified by the parameter δ, which is related with permittivity and temperature as follows (Kirillov and Isupov 1973):

$$\frac{1}{\varepsilon'} - \frac{1}{\varepsilon'_m} = \frac{(T - T_m)^2}{2\varepsilon_m \delta^2}, \tag{5}$$

δ parameter of two different frequencies are calculated by fitting permittivity–temperature data and are 221·5 for 50 kHz and 217·9 for 100 kHz and the fitting as shown in figure 6.

The diffusivity (γ) parameter is applied to characterize the relaxor behaviour and it is expressed by a modified Curie–Weiss law (Uchino and Nomura 1982)

$$\frac{1}{\varepsilon'} - \frac{1}{\varepsilon'_m} = \frac{(T - T_m)^\gamma}{C}, \tag{6}$$

where γ and C are constants for diffusion factor and Curie–Weiss constants, respectively. In general, the diffusion factor is between 1 and 2, representing the normal ferroelectric

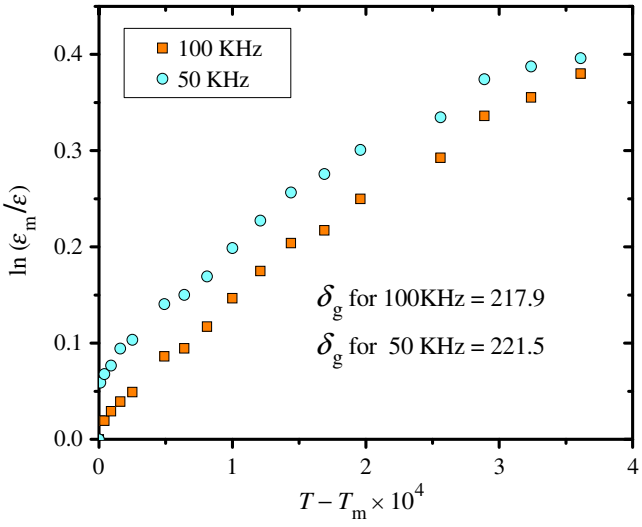

Figure 6. ln $(\varepsilon_m/\varepsilon)$ vs $(T - T_m)$ for 50 kHz and 100 kHz of BNT ceramic.

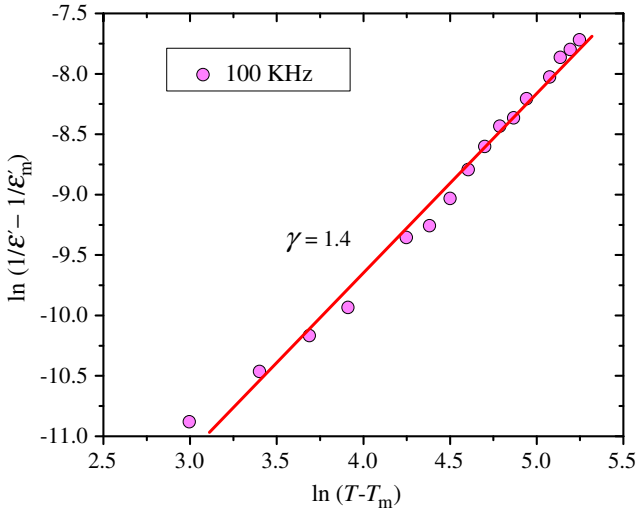

Figure 7. $\log(1/\varepsilon' - 1/\varepsilon_m)$ vs $\log(T - T_m)$ of BNT ceramic at 100 kHz.

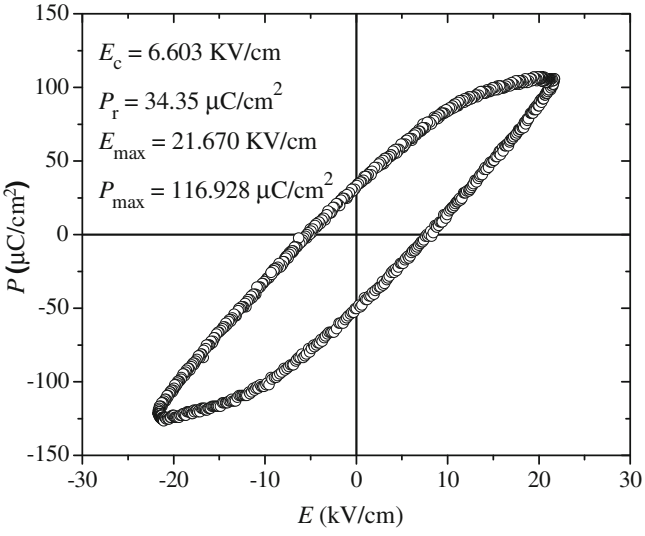

Figure 8. P–E hysteresis loop of BNT ceramic.

phase transition and completed diffusion phase transition. In the case of $\gamma = 1$, a normal Curie–Weiss law is obtained. The diffusion factor can be employed to describe the diffusion phase transition. The plots of $\ln\left(1/\varepsilon' - 1/\varepsilon'_m\right)$ as a function of $\ln(T - T_m)$ for the BNT samples are shown in figure 7. The diffusion factor was found to be 1·4 at 100 kHz.

Figure 8 shows the room temperature P–E hysteresis loops of BNT ceramics sintered at 1150°C. The P–E hysteresis loop indicated that the sample exhibited typical ferroelectric nature. The remnant polarization (P_r), maximum polarization (P_m) and coercive field (E_c) of unpoled BNT ceramic evaluated from the saturated ferroelectric hysteresis loop is summarized in figure 8. The dynamic piezoelectric coefficient (d_{33}) was calculated as the ratio of the maximum strain to the maximum field in the cycle (S_{max}/E_{max}). The strain and dynamic piezoelectric constant d_{33} is 41 pCN^{-1}.

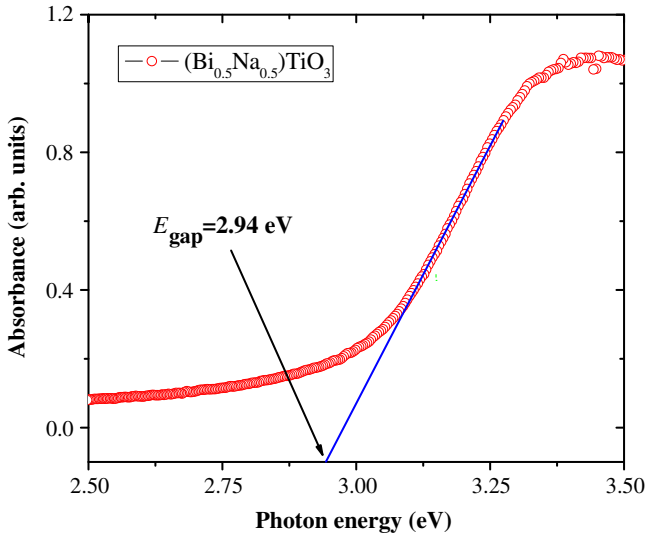

Figure 9. UV–Visible spectrum of BNT powder.

3.4 *Ultraviolet–Visible absorption spectroscopy analyses*

Figure 9 shows the UV–Vis absorbance spectrum of BNT ceramic prepared by solid state reaction (SSR) and sintered at 850°C for 2 h. The optical band gap energy (E_{gap}) was estimated by the method proposed by Wood and Tauc (1972). According to these authors the optical band gap is associated with the absorbance and photon energy by the following equation:

$$h\nu a \propto \left(h\nu - E_{gap}\right)^n, \tag{7}$$

where α is the absorbance, h the Planck constant, ν the frequency, E_{gap} the optical band gap and n is a constant associated with different types of electronic transitions ($n = 1/2$, 2, 3/2 or 3 for direct allowed, indirect allowed, direct forbidden and indirect forbidden transitions, respectively). Thus, the E_{gap} value of BNT ceramic was evaluated extrapolating the linear portion of the curve or tail. In our work, the UV–Vis absorbance spectrum suggests an indirect allowed transition and, therefore, the $n = 2$ was used in (7).

In principle, we believe that the obtained E_{gap} value for the BNT ceramic can be associated to a structural order–disorder effect into the lattice due to a symmetry break between the O–Ti–O bonds and/or distortions on the (TiO_6) clusters. A possible explanation for the origin of this symmetry break can be related with the synthesis method. It is possible to conclude on this hypothesis that the high temperatures employed in the SSR during the sintering process are not sufficient to avoid the presence of structural defects (symmetry break between bonds or distortions) into the BNT structure, mainly those arising from the repeated cycles of grinding.

4. Conclusions

Lead-free BNT ceramics were synthesized successfully using the solid-state reaction route and its structure, microstructure, dielectric, ferroelectric and electric field-induced strain behaviour were investigated. XRD revealed the existence of rhombohedral phase. The sample was sintered at different temperatures. It was shown that sample sintered at 1150°C has the highest density. The dielectric study of the sample sintered at 1150°C reveals diffuse phase transition. BNT ceramics sintered at an optimal temperature of 1150°C showed ferroelectric behaviour at room temperature. The piezoelectric coefficient was found to be (d_{33} = 41 pm/V). The optical property was studied by UV–Vis spectroscopy.

Acknowledgements

The authors would like to thank Prof. T P Sinha, Bose Institute, Kolkata, for extending the facility of dielectric measurements.

References

Diasa A, Vicente T, Buonoa L, Virgínia S, Ciminellia T and Moreira R L 1999 *J. Eur. Ceram. Soc.* **19** 1027
Fullman R L 1953 *Trans. TMS–AIME* **197** 447
Herabut A and Safari A 1997 *J. Am. Ceram. Soc.* **80** 2954
Hiruma Y, Nagata H and Takenaka T 2006 *Jpn. J. Appl. Phys.* **45** 7409
Hiruma Y, Yoshii K, Nagata H and Takenaka T 2008 *J. Appl. Phys.* **103** 84121
Jiang A Q, Li G H and Zhang L D 1997 *Solid State Commun.* **104** 709
Kimura T, Takahashi T, Tani T and Saito Y 2004 *Ceram. Int.* **30** 1161
Kirillov V V and Isupov V A 1973 *Ferroelectrics* **5** 3
Kuharuangrong S and Suhulze W 1996 *J. Am. Ceram. Soc.* **79** 1273
Lenka M M, Oledzka M and Riman R E 2002 *Chem. Mater.* **12** 1323
Liu P, Ma J L, Meng L, Li J, Ding L F, Wang J L and Zhang H W 2009 *Mater. Chem. Phys.* **114** 624
Marcos F R, Ochoa P and Fernandez J F 2007 *J. Eur. Ceram. Soc.* **27** 4125
Perantie J, Hagberg J, Uusimaki A and Jantunen H 2008 *Appl. Phys. Lett.* **93** 132905
Rahaman M N 2003 *Ceramic processing and sintering* (CRC Press) 2nd edn
Said S and Mercurio J P 2001 *J. Eur. Ceram. Soc.* **21** 1333
Smolenskii G A, Agranovskaya A I and Krainic N N 1961 *Sov. Phys. Solid State* **2** 2651
Takenaka H and Takenaka T 1998 *Jpn. J. Appl. Phys.* **37** 5311
Uchino K and Nomura S 1982 *Ferroelectrics* **44** 55
Walsh C J and Schulze W A 2004 *IEEE International Ultrasonics, Ferroelectrics and Frequency Control Joint 50th Anniversary Conference*, 10.1109/ISAF.2004.1418310
Watcharapasorn A, Jiansirisomboon S and Tunkasiri T 2007 *Mater. Lett.* **61** 2986
Wood D L and Tauc J 1972 *Phys. Rev.* **B5** 3144
Zhao P, Zhang B P and Li J F 2007 *Appl. Phys. Lett.* **90** 242909
Zhen Y and Li J F 2006 *J. Am. Ceram. Soc.* **89** 3669
Zvirgzds J V, Kapostis P P and Kruzina T V 1980 *Ferroelectrics* **40** 75